

UNCLASSIFIED

Defense Technical Information Center
Compilation Part Notice

ADP014100

TITLE: Fan Tone Generation and Radiation System

DISTRIBUTION: Approved for public release, distribution unlimited
Availability: Hard copy only.

This paper is part of the following report:

TITLE: Aging Mechanisms and Control. Symposium Part A -
Developments in Computational Aero- and Hydro-Acoustics. Symposium
Part B - Monitoring and Management of Gas Turbine Fleets for Extended
Life and Reduced Costs [Les mecanismes vieillissants et le controle]
[Symposium Partie A - Developpements dans le domaine de
l'aeroacoustique et l'hydroacoustique numeriques] [Symposium Partie B ...

To order the complete compilation report, use: ADA415749

The component part is provided here to allow users access to individually authored sections of proceedings, annals, symposia, etc. However, the component should be considered within the context of the overall compilation report and not as a stand-alone technical report.

The following component part numbers comprise the compilation report:
ADP014092 thru ADP014141

UNCLASSIFIED

Fan Tone Generation and Radiation System

Djaffar Ait-Ali-Yahia, Alexandre Jay and Hany Moustapha

E-Mails: Djaffar.Ait-Ali-Yahia@pwc.ca, Alexandre.Jay@pwc.ca and Hany.Moustapha@pwc.ca

Pratt & Whitney Canada, Department of Acoustics and Installations

1000 Marie-Victorin (01PA4), Longueuil, Quebec, Canada J4G 1A1

1. INTRODUCTION

Designing modern turbofan engines with higher bypass ratios is significantly limited by increasingly restrictive airport noise regulations. Independent of takeoff, cruise or landing operations, the fan rotor-stator interactions remain as one of the major engine sources of noise. Therefore, interest in understanding, modeling and eventually reducing this noise has increased the need for advanced Computational Aero-Acoustics (CAA) codes to serve as a primary tool in the fan design process.

Two years ago, Pratt & Whitney Canada (PWC) initiated a research effort to develop a fan tone generation and radiation system. As displayed in figure 1, this system integrates three in-house computational tools: a CFD fan analysis code such as NS3D, a CAA linear and nonlinear radiation codes, and a fan tone generation module which serves as a link between these CFD and CAA codes.

NS3D is a PWC proprietary code which solves the 3D Navier-Stokes equations for turbomachinery and external flow problems by using an SUPG finite element method on structured and unstructured grids. The development and the validation of this code was already dealt with in reference [1] and here will be mainly used to perform 3D unsteady rotor-stator analyses of fan stages. Therefore, the present paper focuses on the development of a noise generation module which computes the incident fan tone modes, as well as on the validation of the PWC CAA codes that serve in the propagation of the noise sources to the far-field.

Both axisymmetric, nonlinear and linear CAA codes [2,3] were developed for noise radiation from aircraft engines and, more specifically, for fan tone radiation computations. The nonlinear in-house codes, based on the Euler equations with a multidomain spectral method in space and an explicit 2N-storage Runge-Kutta in time, were first developed to achieve a more complete modelling of sound propagation phenomena. However, for typical industrial applications with high frequency incoming spinning modes, the nonlinear code is still demanding in terms of computer resources and it is limited to axisymmetric incident modes.

An intermediate approach has been developed by Eversman [4] that uses a linear modelling of sound propagation in which the mean-flow computation is decoupled from the acoustic field prediction. The methodology involves the solution in an axisymmetric frame of an incompressible potential equation for the mean-flow field and a linearized potential equation in the frequency domain for the acoustic field. Both equations are numerically discretized by a Galerkin finite element method with a direct solution of the resulting linear system of equations.

Although this approach is attractive for fan noise design purposes, it may eventually become prohibitive for acoustic modes with high frequencies. In fact, an accurate prediction of noise propagation with quadratic isoparametric elements requires a fine mesh spacing, with at least six to seven elements (equivalent to between 13 to 15 points) per wavelength. The demand on computer resources is further increased by the use of direct matrix solvers.

In the present paper, a fan tone generation procedure which is based on a high accurate spectral method is presented. The linear acoustic model [4] is also revisited with several numerical and implementation improvements. Finally, several relevant benchmarks are included to demonstrate the efficiency and the accuracy of the current fan tone system.

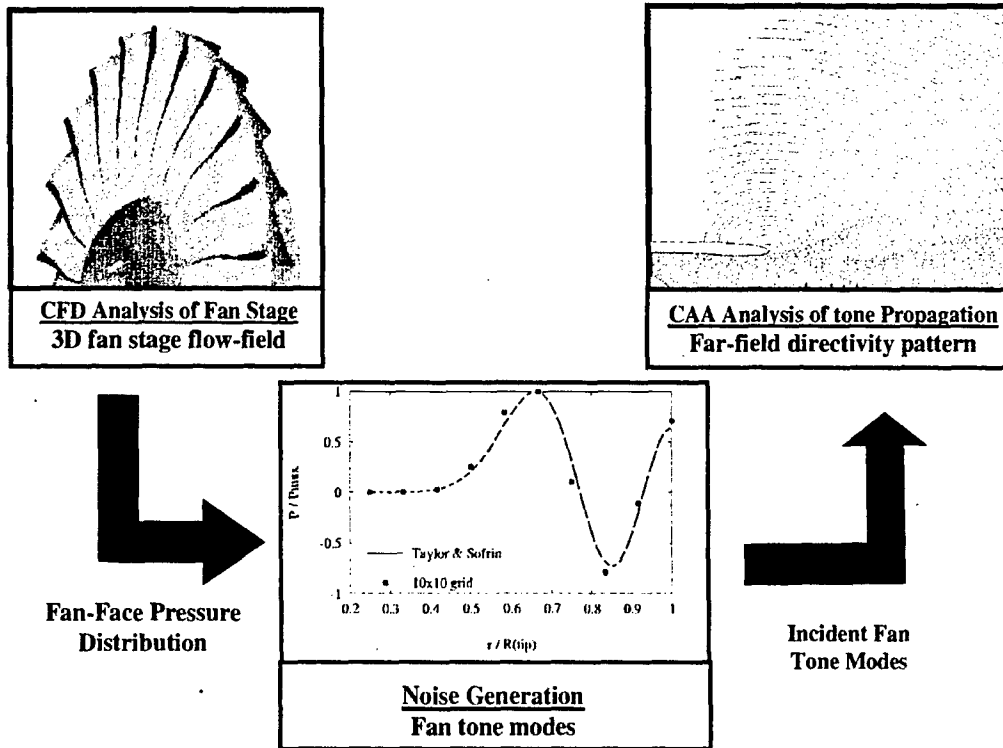


Figure 1. Fan Tone Generation and Radiation System

2. FAN TONE GENERATION

2.1 Methodology

For an infinite annular duct, the general pressure solution for wave propagation in the positive z direction associated with a source located in the plane $z=0$ is given by

$$p(r, \theta', z, t) = \sum_{n=1}^{+\infty} \sum_{m=-\infty}^{+\infty} \sum_{\mu=0}^{+\infty} P_{m\mu}^n E_m^n(\kappa_{m\mu} r) \exp[i(m\theta' - k_{m\mu}^n z - nB \Omega t)] \quad (1)$$

where (r, θ', z) are the cylindrical coordinates in an absolute frame of reference, t is the time variable, n is the index of harmonic of BPF, m is the circumferential mode order, μ is the radial mode order, $P_{m\mu}^n$ is the pressure amplitude for the mode (m, μ) and harmonics n . In general $P_{m\mu}^n$ has a complex value.

E_m is the radial characteristic function or eigenfunction, and $\kappa_{m\mu}$ is the radial eigenvalue. Both these variables are computed by solving an eigenvalue problem subject to a Neumann boundary condition at the inner and outer duct walls. The variable $k_{m\mu}$ represents the axial wave number, which if real, corresponds to a propagating or a cut-on mode and, if complex, describes exponential decay or a cut-off mode.

The angular velocity, ω , of mode m is given by $\omega = n B \Omega / m$, where B represents the blade count and Ω is the shaft rotation frequency. Spinning modes can be generated by rotor-stator interactions or by a rotor alone. In both cases, the circumferential mode order m can only take some discrete values that are dictated by $m = nB + jV$, where B and V are the blade and vane counts, and j is any positive or negative integer.

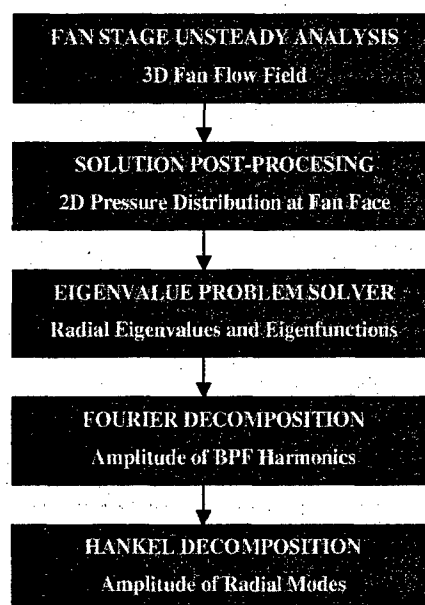


Figure 2. Numerical algorithm of pressure modal expansion for a single harmonic

The numerical algorithm for fan tone generation is summarized in figure 2. Starting from a fan stage solution that could be provided by a CFD analysis code, the pressure field is interpolated into a reference plane which corresponds to the starting boundary (inlet boundary) for the acoustic calculations. This plane covers the blade passage area and is meshed with a 2D polar, uniform grid. The location of this reference plane as well as the size of its grid have a significant impact on the accuracy of predicted noise levels and therefore special care should be taken in their definitions. In general, the reference plane must be sufficiently far from the hydrodynamic field of the rotor blade, where large, non-propagation pressure variations caused by large fluid velocities in the vicinity of the blades may be present. Concerning the grid size, sufficient points should be used in the circumferential and radial directions in order to resolve the high frequencies as well as high radial modes contributions. The optimal number of points in both the circumferential and radial directions will be suggested in the validation section.

Once the acoustic pressure distribution is known on the reference plane, an FFT (Fast Fourier Transform) algorithm is used to compute the contribution of each circumferential mode m . The radial eigenvalue and eigenfunctions are then evaluated by solving a Bessel equation. The Bessel equation is discretized using a

Galerkin spectral element method and the resulting algebraic system of equations is solved by an iterative CG method. It should be noted that the eigenvalue problem depends solely on the circumferential index, m , and the hub to tip ratio, σ . The last step involves the calculation of mode amplitudes $P_{m\mu}$ by performing a Hankel expansion. The evaluation of integrals is carried out numerically using a spectral interpolation within each element.

2.2 Validation

In order to validate the proposed modeling and the accuracy of its numerical implementation, a fan stage with 16 blades and 32 vanes was considered. A pressure distribution made of a uniform mean-flow and the superposition of the first four radial modes ($m=16, \mu=0-3$) is assumed on the reference plane.

Assuming that only the circumferential mode $m=16$ (corresponding to the first harmonics and $j=-1$) can propagate, the acoustic pressure takes the following analytical form

$$p(r, \theta) = \sum_{\mu=0}^3 P_{m\mu} \left[J_m(\kappa_{m\mu} r) + Q_{m\mu} Y_m(\kappa_{m\mu} r) \right] \exp(im\theta) \quad \text{with } m=16 \quad (2)$$

where the constants are defined in Table 1.

μ	$\kappa_{m\mu}$	$Q_{m\mu}$	$P_{m\mu}$
0	18.063	0.000	0.600
1	23.264	0.000	0.300
2	27.347	0.000	0.200
3	31.111	0.000	0.100

Table 1. Definition of pressure expansion constants.

The iso-contours of this non-dimensional pressure distribution is displayed in figure 3-(left) while the acoustic contribution is illustrated in figure 3-(right). The reference plane is chosen at an axial position where the hub to tip ratio $\sigma=0.25$. This plane was meshed with different densities to investigate the grid dependency. The present validation work includes a coarse grid with 10x10 points, a medium grid with 20x20 points and a fine grid with 40x40 points per blade passage.

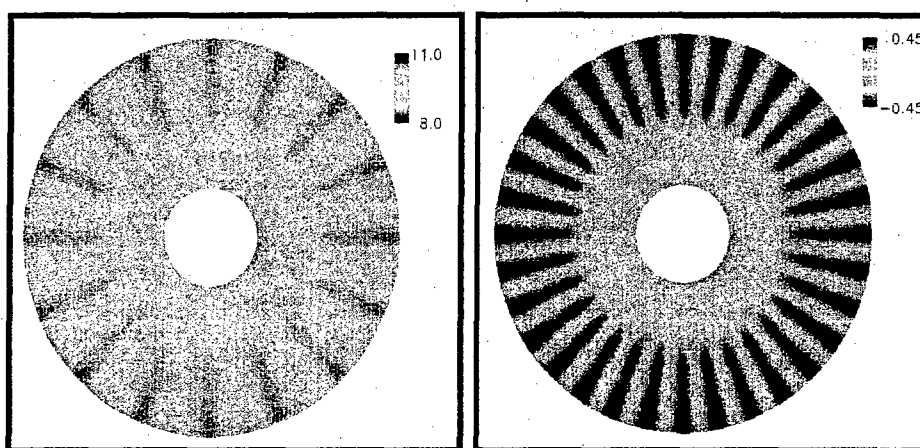


Figure 3. Iso-contours of non-dimensional pressure distribution (left) and its acoustic component (right).

Table 2 displays a comparison between the computed eigenvalues and, Tyler and Sofrin results [5]. It is observed that the predictions become less accurate as the radial index increases. It is also noticed that the grid with 10x10 points gives a 5% relative error for the highest considered radial mode while the use of a finer grid with 40x40 points lowers this error to 0.5%.

Radial Mode	Computed $\kappa_{m\mu}$			Tyler & Sofrin [5]
	10x10 points	20x20 points	40x40 points	
0	18.1102	18.0742	18.0659	18.063
1	23.5700	23.3366	23.2816	23.264
2	28.1608	27.5464	27.3954	27.347
3	32.6645	31.5100	31.2086	31.111

Table 2. Comparison between computed $\kappa_{m\mu}$ with Taylor & Sofrin results [5].

The computed eigenfunctions are compared against Sofrin & Taylor results [5] for different grid density in figure 4. It is clear that the grid with 10x10 points is not capable of resolving the shape of high radial modes such as $\mu=2$ or 3. On the other hand, the finest grid with 40x40 points leads to accurate description of all considered radial eigenfunctions.

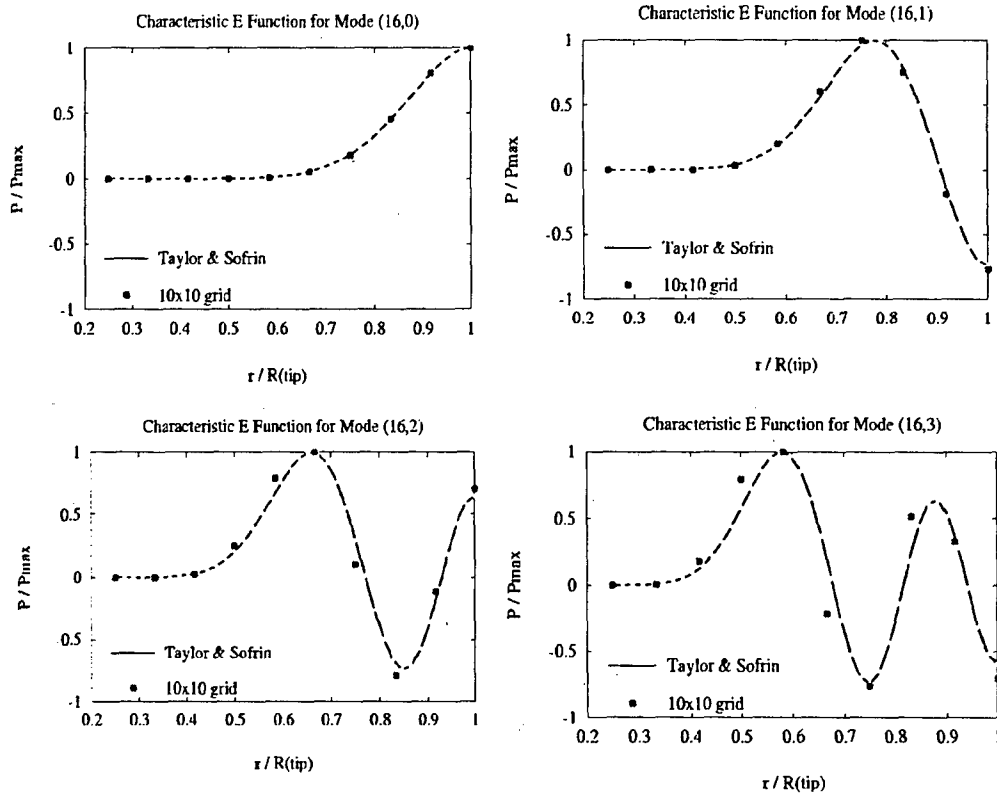


Figure 4. Characteristic E Functions (radial eigenfunction):
Comparison of predictions vs Tyler & Sofrin results for different grid densities

The FFT of the acoustic pressure distribution in the circumferential direction yields to Fourier coefficients \hat{P}_m at each grid radial station. The histogram displayed in figure 5 shows that magnitude of Fourier coefficients $|\hat{P}_m|$ are only different from zero for the circumferential mode $m=16$, which is consistent with the assumed acoustic pressure given by the equation (2).

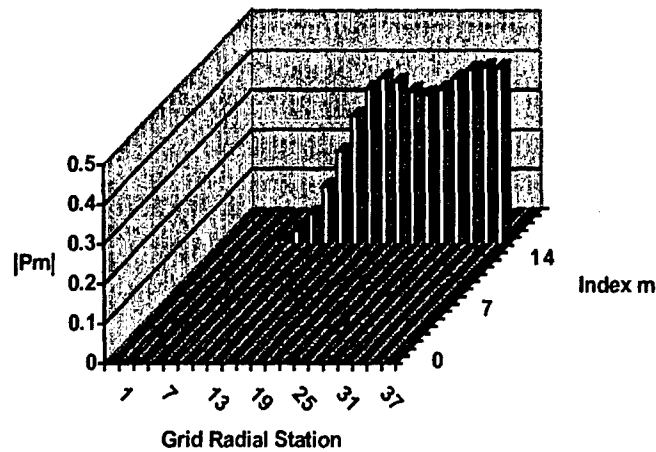


Figure 5. Fourier expansion of the pressure distribution on the finest grid.

Using these Fourier coefficients \hat{P}_m , a Hankel decomposition is performed in the radial direction to compute the contribution of each radial mode. The comparison of computed amplitudes $|P_{mu}|$ against the exact values given by Table 1 is presented in figure 6. It can be seen that the coarse grid with 10x10 points predicted poorly the amplitude of higher radial modes while the finer grid with 40x40 points allows better match to the exact values.

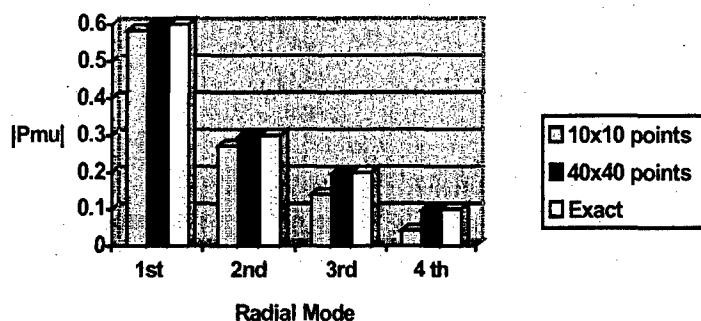


Figure 6. Comparison of computed amplitudes against exact values.

3. FAN TONE PROPAGATION

3.1 Methodology

The present methodology presents several numerical and implementation improvements to the linear acoustic model [4]. The mean-flow modelling is upgraded to the full potential equation. This is expected to improve predictions of the radiated sound field because the refraction effects, which occur mainly in the region of the inlet aperture, are accounted for. Spectral elements are used for space discretization, which brings down the number of necessary points per wavelength to between four and five for a sufficiently large number of Gauss-Chebyshev-Lobatto (GCL) points per element. The treatment of radiation boundary is drastically improved through a damping layer which better preserves phase information in the computational domain. The resulting algebraic systems of equations can be solved either by direct or iterative solvers, which are optimized on distributed memory machines through the use of the PETSc (Portable, Extensible Toolkit for Scientific Computations) library [6].

Finally, GCL grids are systematically generated using a CAD based approach [7] embedded within the aeroacoustic code. These grids may also be dynamically adapted by varying the number of GCL points per element as a function of blade passing frequency to yield the minimum number of points per wavelength needed to guarantee a certain level of accuracy.

3.2 Validation

A/ Radiation from a Semi-Infinite Cylinder

The acoustic solver is first tested on a sound radiation problem with no mean-flow from a semi-infinite cylinder of zero wall thickness, as displayed in figure 7. This test case is chosen due to the availability of an exact analytical solution.

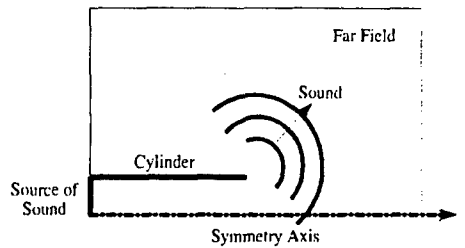


Figure 7. **Semi-infinite cylinder:** definition of sound radiation problem.

- The radiation of the plane wave (0,0) and the first radial (0,1) modes are considered in the axisymmetric case, $m=0$, and with a reduced frequency of 10.3. The domain was partitioned into 162 elements and the number of GCL points was varied between 6 and 8. This corresponds to a number of points per wavelength, $N_\lambda=5$.

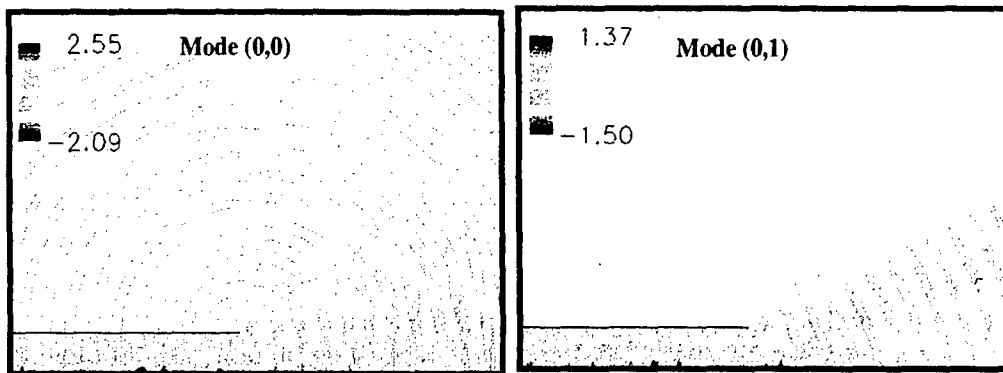


Figure 8. **Semi-infinite cylinder:** Contours of the real part of the acoustic pressure.

Once the complex acoustic pressure variable (real part is displayed in figure 8) is deduced from the acoustic potential, the amplitude of the acoustic pressure is computed by taking the module of the complex variable. The display of the amplitude of the acoustic pressure in figure 9 shows the existence of three main lobes.

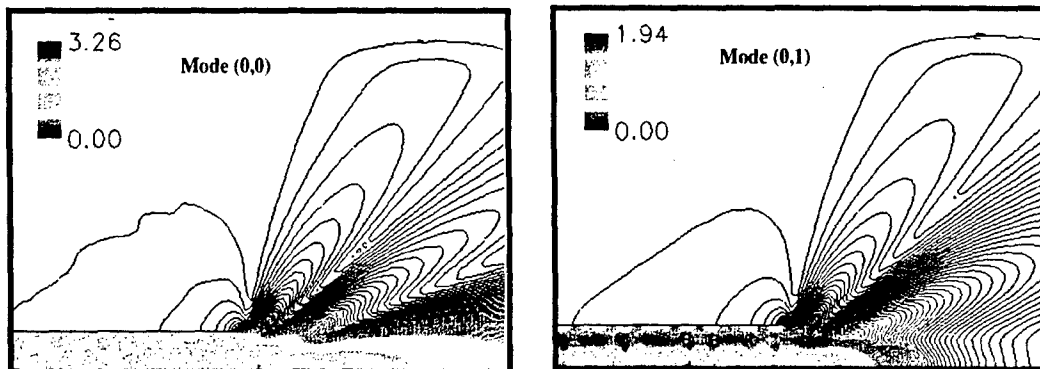


Figure 9. **Semi-infinite cylinder:** Contours of the amplitude of the acoustic pressure.

Figure 10 compares the computed sound pressure level (SPL) directivity in the far field against the analytical solution for radiation from a plane circular piston, vibrating in the same mode, as obtained by Tyler and Sofrin [5]. The agreement between the computation and the analytical result is excellent except at very high angles. This is expected since at these angles the influence of the walls, which the analytical solution does not account for, is more important.

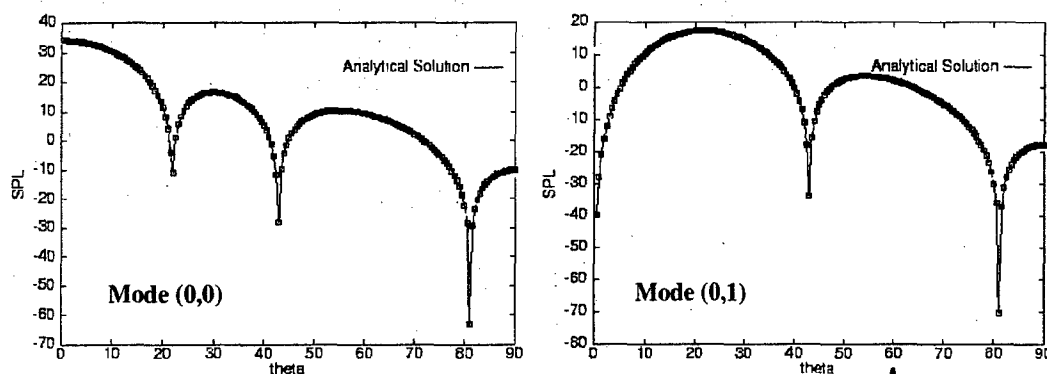


Figure 10. Semi-infinite cylinder: SPL directivity patterns.

B/ Fan Tone Radiation from the PW545 Inlet

The propagation code is also tested on the PW545 turbofan inlet with no mean-flow for the incoming spinning modes: BPF (0,0) and BPF (0,1). The angular speed is set to 12,000 rpm leading to a BPF of 3800Hz and a reduced frequency of 24.4.

Far field directivity patterns which are computed by linear and nonlinear analyses are compared in figure 11. Overall, a good agreement is observed between the linear and nonlinear predictions. This was expected since nonlinear effects were minimized in by considering a no mean-flow case and small acoustic amplitudes.

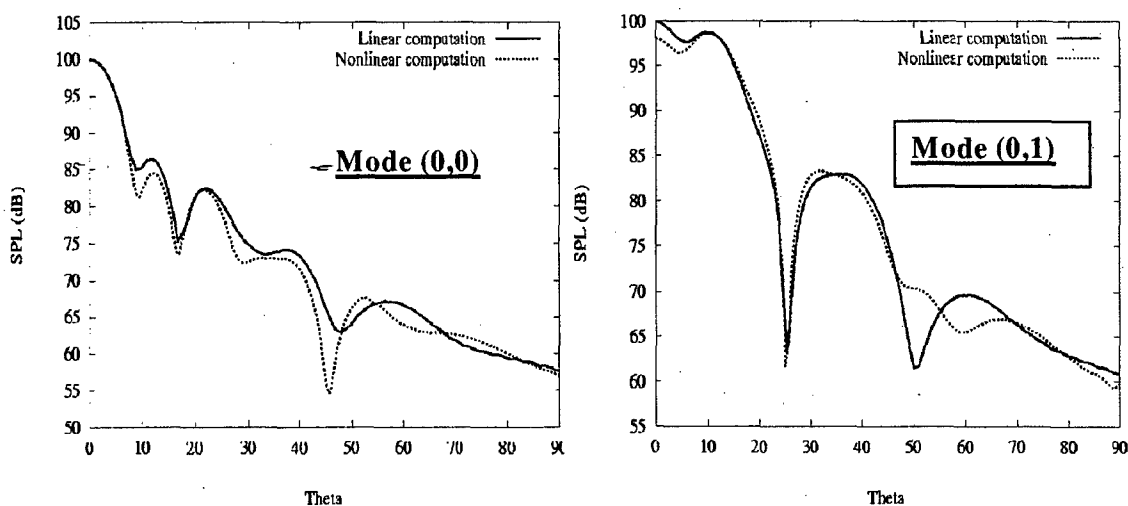


Figure 11. PW545 inlet: Far field directivity patterns using linear and nonlinear models.

The nonlinear acoustic solver was time marched until $t=30$ in order to achieve a periodic solution, necessitating around 11,000 iterations. This required 2 hours on four R10000 CPUs of an SGI Origin 2000 computer. On the other hand, the present linear acoustic solver required a single iteration or 7 minutes on a single R10000 CPU.

The effect of the mean-flow on the fan noise radiation is studied for the BPF (0,1) mode. The mean-flow is first computed for the far-field Mach number of 0.2 and a mass flow rate of 30 kg/s and then an acoustic calculation is performed for the first radial mode with a nondimensional acoustic source amplitude of 0.01.

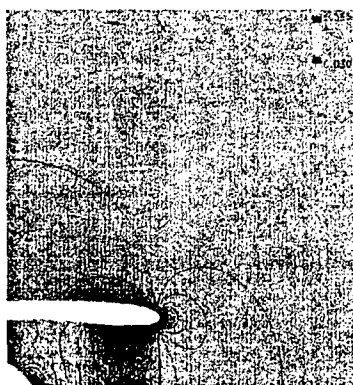


Figure 12. **PW545 inlet:** Mach number contours of the mean-flow.

The mean-flow solution is displayed in figure 12 as Mach number contours. A maximum Mach number of 0.26 is reached at the throat. The resulting radiation directivity pattern is compared with the corresponding no forward flight (i.e. no mean-flow) case in figure 13. This plot shows a reduction of 10 dB in the principal lobe.

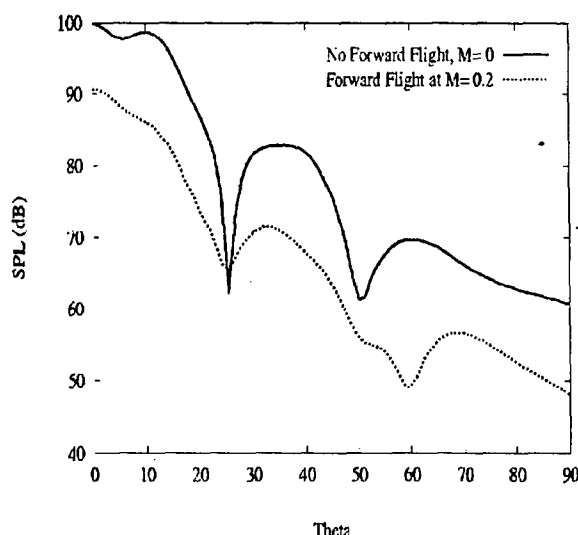


Figure 13. **PW545 inlet:** effect of forward flight speed on the directivity pattern.

C/ Fan Tone Radiation from the JT15D Inlet

In-flight measurements of the noise radiated from a modified JT15D-1 inlet have been presented by Preisser *et al* in reference [8]. The JT15D-1 is a small turbofan engine with 28 fan blades. An array of 41 small diameter rods have been installed on the casing of the nacelle, such that their interactions with the 28 fan blades generate modes with a circumferential order of 13 turning at BPF.

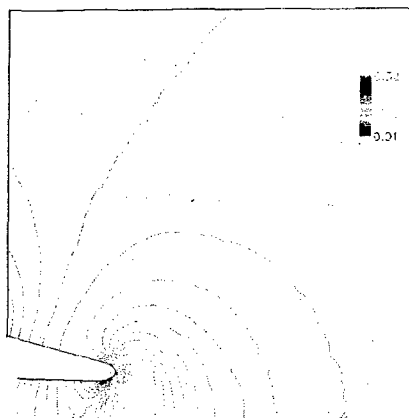


Figure 14. JT15D inlet at 8010 RPM: Mach number contours of the mean-flow.

In the considered case, only the mode (13,0) is above cut-off. Boundary conditions have been specified in terms of the mass flow rate at the fan face, set to 16.6 kg/s, and the far field Mach number of 0.204. The contours of the mean-flow Mach number are illustrated in figure 14. SPL contours, displayed in figure 15, look smooth and free of numerical reflections that could be generated by the far field boundary. This figure also shows the existence of a major lobe at an angle of 55 degrees with a maximum SPL of 170 dB.

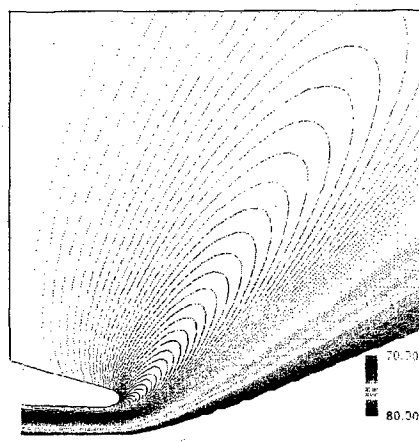


Figure 15. JT15D inlet at 8010 RPM: SPL contours.

The computed directivity is compared with the experimental data in figure 16. We observe that the predicted directivity radiates at a slightly larger angle than the measured one.

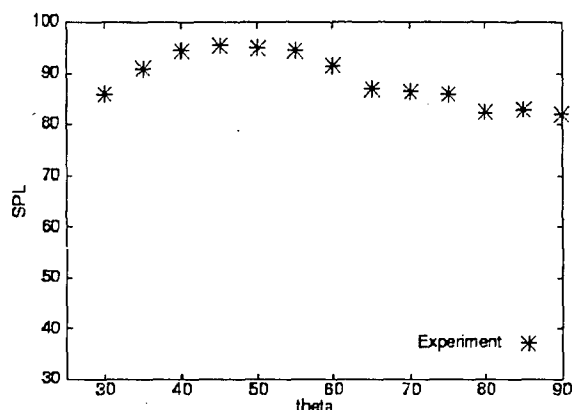


Figure 16. JT15D inlet at 8010 RPM: SPL directivity.

4. CONCLUSIONS

A fan tone generation and radiation system was presented. A computational module for fan tone generation has been developed and validated to serve as a link between any CFD fan analysis code and the in-house CAA radiation codes. The fan tone propagation codes were also validated on several generic and industrial benchmarks. These test cases demonstrate the potential of the present system for becoming an effective tool in performing a wide range of parametric studies for fan acoustic design.

5. REFERENCES

1. Tam, A., Ait-Ali-Yahia, D., Robichaud, M.P., Moore, M., Habashi, W.G., "Anisotropic Mesh Adaptation for 3D Flows on Structured and Unstructured Grids", *Journal of Computer Methods in Applied Mechanics and Engineering*, vol. 189, PP. 1205-1230, 2000.
2. Stanescu, D., Ait-Ali-Yahia, D., Habashi, W.G. and Robichaud, M., "Multidomain Spectral Computations of Sound Radiation from Ducted Fans", *AIAA Journal*, Vol. 37, No. 3, 1999, pp. 296-302.
3. Stanescu, D., Ait-Ali-Yahia, D., Habashi, W.G. and Robichaud, M.P., "Galerkin Spectral Element Method for Fan tone Radiation Computations", 6 th AIAA/CAES Aeroacoustics Conference, AIAA 2000-1912, June 12-14, 2000, Lahaina, Hawaii, USA.
4. Roy, I.D., Eversman, W., and Meyer, H.D., "Improved Finite Element Modeling of the Turbofan Engine Inlet Radiation Problem", NASA Report, Contract NAS3-25952, April 1993.
5. J.M. Tyler and T.G. Sofrin, "Axial Flow Compressor Noise Studies", *SAE Transactions*, Vol. 70, pp. 309-332.
6. Balay, S., Gropp, W.D., McInnes, L.C., and Smith, B.F., "PETSc User Manual", ANL-95/11, Revision 2.0.24, Argonne National Laboratory, 1999.
7. D. Ait-Ali-Yahia, D. Stanescu, M. Robichaud and W.G. Habashi, "Spectral Element Grid Generation and Nonlinear Computations for Noise Radiation from Aircraft Engines", *AIAA Paper 99-1832*, May 1999, Seattle, WA, USA.
8. Preisser, J.S., Silcox, R.J., Eversman, W., and Parrett, A.V., "A Flight Study of Tone Radiation Patterns Generated by Inlet Rods in a Small Turbofan Engine", *AIAA Paper 84-0499*, Jan. 9-12, 1984, Reno, Nevada.